Hormone-induced thrombosis is mediated through non-canonical fibrin(ogen) aggregation and a novel estrogen target in zebrafish

Xinge Yu[1]*, Murat Yaman[1]*, Queena Y. Zhao[1], Sylvia M. Emly[1], Jacqueline K. Lee[1], Hongyu Su[2], Allison C. Ferguson[1], Chandrasekaran Nagaswami[3], Saireudee Chaturantabut[4], Wolfram Goessling[4-8], John W. Weisel[3], Richard J. Auchus[2,9], Jordan A. Shavit[1,10]

[1] Department of Pediatrics, University of Michigan, Ann Arbor, MI

[2] Department of Pharmacology, University of Michigan, Ann Arbor, MI

[3] Department of Cell and Developmental Biology, University of Pennsylvania School of Medicine, Philadelphia, PA

[4] Division of Genetics, Brigham and Women's Hospital, Harvard Medical School, Boston, MA

[5] Broad Institute of MIT and Harvard, Cambridge, MA

[6] Harvard Stem Cell Institute, Cambridge, MA

[7] Division of Health Sciences and Technology, Harvard-MIT, Cambridge, MA

[8] Division of Gastroenterology, Massachusetts General Hospital, Boston, MA

[9] Department of Internal Medicine, University of Michigan, Ann Arbor, MI

[10] Department of Human Genetics, University of Michigan, Ann Arbor, MI

Correspondence: Jordan A. Shavit, Department of Pediatrics, University of Michigan, Room 8301, Medical Science Research Building III, 1150 West Medical Center Dr, Ann Arbor, MI 48109; email: jshavit@umich.edu

* XY and MY contributed equally to this work.

23 **Conflict of interest disclosures**

24 J.A.S. has been a consultant for Sanofi, NovoNordisk, Biomarin, Takeda, Pfizer, Genentech, CSL

25 Behring, and Medexus. The other authors declare no relevant conflicts of interest.

26

Abstract

Venous thrombosis is a well-known complication of estrogen exposure, with nearly every woman at risk across her lifetime through contraception, pregnancy, or hormone therapy. Although estrogens alter expression of coagulation factors, the mechanisms that mediate estrogen-induced thrombosis are poorly understood, partially due to the absence of an animal model. Identification of these mediators is central to understanding of hormone-induced pathophysiology, could ascertain patients at higher risk for thrombosis, and pinpoint future therapeutic targets. The zebrafish is characterized by external development, high fecundity, optical transparency, and hemostasis is highly conserved with humans. Through a transgenic line that generates GFP-tagged fibrinogen, we show rapid onset of thrombosis after exposure to various estrogens, but not progestins or testosterone. Thrombi are localized to the venous system with evidence for clot contraction. Thrombosis is only partially impeded by anticoagulants, occurs in the absence of factor VII, factor X, and prothrombin, but is dependent on tissue factor and fibrin(ogen). Finally, targeting of all known estrogen receptors does not eliminate thrombosis. The inability to completely inhibit thrombosis through genetic/pharmacologic anticoagulation or estrogen receptor disruption suggests mechanisms different from canonical coagulation/thrombosis. These studies suggest that estrogen-induced thrombosis is a unique entity distinct from other forms of venous thrombosis.

45 # Introduction

46 Venous thromboembolism (VTE) is caused by the formation of pathologic blood clots in major
47 veins, resulting in deep vein thrombosis and/or pulmonary embolism. According to the Centers
48 for Disease Control, VTE affects ~900,000 people/year in the U.S., and accounts for 60,000-
49 100,000 deaths (1). Major causes are inherited or acquired hypercoagulable states and estrogen
50 exposures, the latter most prominently from combined oral contraceptives (COCs) (1-3), but
51 also including pregnancy and hormone replacement therapies. Estrogen is a longstanding well-
52 known risk factor for VTE (4-6), especially in combination with other acquired risk factors, such
53 as smoking and obesity (7). Despite multiple clinical studies, the mechanisms of estrogen-induced
54 thrombosis are minimally understood (8).

55

56 Estrogens target multiple receptors with various agonistic affinities for both classic nuclear
57 hormone receptors (NHRs, the estrogen receptors (ESRs)) (8) and a G-protein coupled estrogen
58 receptor (GPER1) (9). In premenopausal women, 17α-ethinylestradiol (EE2), a synthetic estrogen
59 with four to five times the potency of natural estrogens, is the one most commonly used in COCs.
60 Activities are also dependent on the crosstalk between various hormone receptors, including
61 progestins, androgens, and estrogens (10). For example, some androgens, such as 19-
62 nortestosterone, have weak estrogenic activities (11), and some progestins are known to have weak
63 androgenic activities (12). Estrogen functions through two mechanisms, genomic and non-
64 genomic (13). ER_{α} and ER_{β} (genes *ESR1* and *ESR2*) are the two NHRs, with zebrafish orthologs
65 Esr1, Esr2a, and Esr2b (14, 15). After interacting with estrogen, these NHRs dimerize and
66 translocate to the nucleus to bind estrogen response elements (EREs) and regulate gene

67 transcription (16). Non-genomic effects are mediated by GPER1 (17). There is also evidence for
68 additional receptors (18, 19), as well as new functions for known NHRs (20, 21).
69
70 Over the years, studies have shown that estrogens are able to upregulate gene expression of
71 multiple blood coagulation factors in humans, mice, and zebrafish (8, 22-24) and to downregulate
72 expression of anticoagulant factors (25, 26). Recent progress has been made through *in vitro* and
73 *ex vivo* studies. In endothelial cells, 17β-estradiol (E2) activates exocytosis through ER_{α} (27), but
74 COCs do not affect endothelial procoagulant activity, even with overexpression of the *ESR* genes
75 (28). *Ex vivo*, E2 appears to affect clot dynamics, including formation, propagation, strength,
76 structure, and fibrinolysis. However, *in vivo* murine studies have been largely unsuccessful, as EE2
77 increases thrombin generation, but there is no increase in tissue fibrin deposition or a visible
78 thrombotic phenotype (29). Additionally, these studies show suppression of thrombosis by EE2
79 (30). Thus, absence of a relevant animal model has contributed to a continued lack of mechanistic
80 understanding.
81
82 As a vertebrate model, zebrafish (*Danio rerio*) exhibits unique characteristics such as external
83 fertilization, rapid development, high fecundity, and optical transparency, and possesses all the
84 key coagulation factors found in humans (31-33). The transparency of zebrafish larvae allows for
85 real-time observation of blood circulation and fluid dynamics. Our previous research utilizing
86 genome editing in zebrafish has revealed remarkable similarities between the pro- and
87 anticoagulant factors in zebrafish and those in humans (34-39). Zebrafish also demonstrate the
88 preservation of major estrogen receptors and estrogen-regulated gene activities (40-42). In this
89 study, we show that zebrafish develop venous thrombosis in response to multiple estrogens, but

90 not progestins or testosterone. These thrombi form even in the absence or inhibition of the
91 coagulation cascade, as well as absence of all known estrogen receptors, although tissue factor (TF,
92 *f3* gene) and fibrin(ogen) are required. These data suggest the presence of alternative pathway(s)
93 for thrombosis, which might involve fibrinogen crosslinking.

94 # Results

95 ***E2 causes thrombosis in vivo***

96 We first tested endogenous estrogen activity by incubating E2 for 5 hours in *fgb-egfp* larvae, and
97 discovered fluorescent thrombi appearing prominently in the posterior cardinal vein (PCV) (Figure
98 1A). A semi-quantitative grading system (Figure 1B) was developed and found to be highly
99 reproducible between independent observers. When we compared these results to quantitative
100 measurement of fluorescence through corrected total cell fluorescence (CTCF), there was strong
101 correlation between the two methods (Spearman's ρ: 0.84, Figure 1C). Given this result and ease
102 of use, all further data were collected using the grading system. The most efficacious results were
103 observed at relatively high concentrations of E2 (50-75 μM). Subsequently, we measured larval
104 plasma concentrations and found that only a small fraction of E2 was absorbed in individual larvae
105 (Figure 1D).

106

107 ***Synthetic estrogens induce in vivo thrombosis***

108 E2 and EE2 (the most common form of estrogen in COCs) both showed dose-dependent induction
109 of thromboses in our model (Figure 2, A and B); however, these findings were inconsistent
110 between experiments. What is shown are the "representative" best data, but often times we found
111 the overall frequency of thrombosis to be less than 50%, even at the high concentrations. Therefore,
112 we evaluated two prodrugs that are metabolized to EE2 *in vivo*, mestranol and quinestrol. These
113 compounds demonstrated greater potency and efficacy, as they were consistent across multiple
114 experiments, although required longer incubations (24-48 hours, Figure 2, C and D).

115

116 ***Testosterone derivatives and progestins do not cause thrombosis***

117 Testosterone has been shown to have an association with increased VTE (43), so we evaluated
118 three testosterone derivatives. None of these showed any significant thrombotic activity (Figure 3,
119 A-C). Progestins are considered to be relatively safe when taken independently (8), and four
120 progestins (at the maximum tolerated doses) across different generations were evaluated, but none
121 of them triggered thrombosis (Figure 3D).
122
123 ***Static and time-lapse imaging of estrogen-induced thrombosis***
124 To confirm the localization and composition of estrogen-induced thrombi, we used confocal and
125 scanning electron microscopy. Confocal imaging was performed in a double transgenic that
126 included *flk-mcherry*, labeling endothelial cells with red fluorescence, along with *fgb-egfp* to
127 identify thrombi. GFP was not colocalized with endothelial cells, indicating its presence in the
128 lumen of the PCV (Figure 4, A and B, and Supplemental Video). Additionally, GFP was not
129 observed in the dorsal aorta (DA), although was occasionally found in the intersegment vessels
130 (ISVs). These details indicate that thromboses were not generated within nor internalized by
131 endothelial cells. Increasing doses or duration of incubation did not result in arterial thrombosis.
132
133 In humans, it is well-known that thrombi often originate at a site of injury, and then extend through
134 the vasculature. However, given the spontaneous and unpredictable nature of estrogen-induced
135 thrombosis, it is unknown how this occurs in patients. Time-lapse imaging was performed over a
136 six-hour period after initiation of treatment with E2. The results show that thrombosis occurs
137 simultaneously across the venous endothelium, rather than initiating and spreading from a single
138 location (Figure 4, C-F). Scanning electron microscope images revealed the morphology of these
139 thrombi in E2-treated larvae (Figure 4, G and H). We observed polyhedrocytes (Figure 4H),

140 consistent with the shape change that occurs in erythrocytes after clot contraction(44, 45). We have
141 previously shown that this process occurs in zebrafish thrombi that develop after induced
142 endothelial injury (46). Sparse fibers were also observed (Figure 4H), which we hypothesize could
143 be composed of fibrin and/or fibrinogen. Given these findings, we evaluated cellular effects of
144 erythrocytes and thrombocytes, and assessed the influence of von Willebrand factor (*vwf*). The
145 *mon*^{tg234} larvae, which lack erythrocytes, surprisingly showed a slightly increased incidence of
146 thrombosis after estrogen exposure, suggesting that red cells potentially buffer against estrogen-
147 induced thrombus formation (Figure 4I). Loss of VWF also did not affect estrogen-induced
148 thrombosis, as *vwf*-null larvae formed wild-type levels of thrombosis (Figure 4J). Using the *cd41-*
149 *egfp* thrombocyte reporter line, we counted thrombocytes that became immobilized in the PCV
150 after mestranol treatment, and there was no difference, indicating a lack of thrombocyte
151 recruitment to the site of thrombi (Figure 4, K and L**).**
152
153 ***Estrogen-induced thrombi are not dependent on the common pathway of coagulation***
154 To further determine the origins of the thrombi, we evaluated coagulation using inhibitors and
155 multiple clotting factor knockout lines. We initially tested several clinical anticoagulants,
156 including warfarin, rivaroxaban (factor Xa inhibitor), and dabigatran (thrombin inhibitor), and
157 knockouts of factor X (*f10*) and prothrombin (*f2*) (35, 39). We have previously shown both the
158 inhibitors and knockouts result in complete loss of induced thrombosis secondary to endothelial
159 injury (34, 35, 39). In contrast, we found that the anticoagulants significantly reduced the intensity
160 and frequency of estrogen-induced thrombosis, but did not completely block its occurrence (Figure
161 5, A and B). Surprisingly, in the *f10* and *f2* knockouts, which would be expected to have no
162 thrombus formation, there was no inhibition of thrombosis in the homozygous mutants (Figure 5,

163 C and D). Given these results, we evaluated whether fibrinogen itself is a component in the
164 observed thrombi by examining estrogen-induced thrombosis in an a-chain (*fga*) knockout.
165 Absence of the a-chain has proven to result in complete loss of fibrinogen in mammals (47-49)
166 and zebrafish (36, 50). We have shown that the *fga* knockout also has complete absence of
167 endothelial injury-induced thrombosis (36). Siblings from $fga^{+/-}$ incrosses were incubated with
168 either E2 or mestranol, and in both cases there was no thrombosis detected (Figure 5, E and F).
169 The *fgb-egfp* line is labeled with GFP on the β-chain, therefore loss of fluorescent thrombi in the
170 a-chain knockout confirms that these are fibrin(ogen)-containing structures rather than non-
171 specific GFP accumulation.
172
173 These data, as well as the time-lapse imaging, suggest that estrogen-induced thrombi may be
174 composed of fibrin and/or fibrinogen, and initiated through endothelial cell signaling. TF is known
175 for cell signaling properties, distinct from its role in coagulation (51). The gene for TF is duplicated
176 in zebrafish, with paralogs *f3a* and *f3b* (52). Larvae devoid of *f3b* showed a ~50% reduction in
177 estrogen-induced thrombosis (Figure 5G). Loss of *f3a* alone had no significant effect, but double
178 knockouts ($f3a^{-/-}$; $f3b^{-/-}$) exhibited an ~80% decrease in thrombosis, demonstrating a prominent
179 role for TF (Figure 5G). Given these data, we hypothesized that loss of factor VII (FVII) would
180 phenocopy TF deficiency. The *f7* gene in zebrafish is triplicated (*f7*, *f7l*, *f7i*) in cis(53), and
181 paralogs are closely related to human FVII (54-56). We and others have found that loss of FVII
182 leads to a partial reduction in induced thrombosis due to endothelial injury (57), but combined
183 deletion of the tandem *f7l*/*f7* locus completely ablates thrombus formation (Shavit laboratory,
184 manuscript in preparation). *f7i* has been shown to be inhibitory rather than procoagulant and thus

185 was not evaluated (56). Surprisingly, examination of estrogen-induced thrombosis showed no
186 effect with loss of FVII activity (Figure 5H).

187 ***Estrogen-induced thrombosis is mediated through a non-canonical target***

188 Next, we explored whether the effect is mediated through known estrogen receptors. We first
189 examined fulvestrant (58), an estrogen antagonist with similar binding affinity to E2. It is simply
190 a 7α-alkylsulphinyl analog of E2 that prevents nuclear hormone receptor dimerization, which is
191 essential for downstream signaling and facilitates receptor degradation. We treated zebrafish
192 larvae with E2 or mestranol and fulvestrant, and observed significant reduction of thrombosis
193 (Figure 6, A and B). We proceeded to examine the effect of loss of the various estrogen receptors,
194 starting with the NHRs (*esr1*, *esr2a*, and *esr2b*). Previous studies with small indels have found that
195 double and triple, but not single mutants have effects on reproduction (59), so we chose to produce
196 complete locus deletions of each gene to ensure complete ablation (Supplemental Figure 1). Since
197 *esr1* and *esr2a* are tightly linked, we had to produce these double mutants through iterative
198 targeting. Using a triple heterozygous mutant incross, we were able to evaluate single *esr2b*,
199 double *esr1/2a*, and triple homozygous mutants (Figure 6C), all of which developed equivalent
200 levels of estrogen-induced thrombosis. The same was true of a G-protein coupled estrogen receptor
201 1 (*gper1*) knockout line (60), which also exhibited persistent thrombosis (Figure 6D). There is
202 evidence for a different membrane-associated GPR in the mouse that responds to estrogen, which
203 is selectively targeted by the synthetic nonsteroidal ligand STX (18, 61). STX treatment in
204 zebrafish demonstrated no effect on thrombosis formation across multiple concentrations up to
205 100 μM (Figure 6E)(18). Taken together, these data suggest the existence of an alternative estrogen
206 target that is distinct from these other known receptors.

207

208 It is well known that 30-40% of zebrafish genes are duplicated due to an ancient event (62). The
209 whole genome has been sequenced (53) and it is believed that there are only three *esr* genes, but
210 the possibility remains that additional ones may exist. A Y549S substitution has been shown to
211 render zebrafish Esr1 constitutively active (63). We cloned *esr1* under control of a ubiquitous
212 promoter (64) and engineered this substitution, but transgenic embryos did not survive (data not
213 shown). Therefore, we swapped in a heat shock promoter to enable activation of *esr1* at selected
214 timepoints, along with a fluorescent *mcherry* reporter (Figure 7A). We injected this construct into
215 the *ere-gfp* transgenic line, which has been shown to be responsive to activated estrogen receptors
216 (41). After heat shock, both *mcherry* and *gfp* signals were observed indicating successful
217 expression of the mutant *esr1* and activation of the *ere-gfp* transgene (Figure 7B). However, when
218 injected into the *fgb-egfp* background, no thrombosis was observed in either group. Taken together,
219 these data suggest that estrogen-induced thrombosis is mediated through a novel target.

220 ## Discussion

221 Thrombosis has been a well-known consequence of estrogen therapy for decades, yet we still know
222 little about the underlying mechanisms. One of the major factors is the lack of an animal model.
223 Blood coagulation is a complex process that relies on circulating cells and proteins in the context
224 of an intact endothelial system, which is not easily modeled *in vitro*. Despite the aforementioned
225 *in vitro* and *in vivo* murine studies, there remain many unanswered questions. We have developed
226 a reliable and genetically tractable model using zebrafish, which has yielded some potential
227 answers. Furthermore, this highly penetrant model that does not require weeks or months to
228 develop a phenotype is a major advantage for future studies. Zebrafish treated with estrogens
229 replicate key characteristics consistent with most human estrogen-induced thromboses, including
230 typical development in the venous rather than arterial system, and lack of thrombosis in response
231 to progesterone. Due to the transparency of zebrafish, we were also able to address a question that
232 is essentially impossible to answer in mammals, i.e., the nature of the initiating event. In humans,
233 thrombosis is often triggered by localized endothelial injury, e.g., trauma, surgery, and vascular
234 access devices. Frequently, these thrombi subsequently spread through the vasculature. Since
235 estrogen-induced thrombosis occurs weeks to months after initiation of therapy, it is difficult to
236 determine if the process is similar. Through time-lapse imaging, we found that thrombosis initiates
237 simultaneously along the venous endothelium. In our companion study, we also observed potential
238 structural differences: estrogen-induced thrombi formed a speckled distribution, while in protein
239 C (PC)-deficient lines (65) thrombi progressed via sprouting patterns with occasional dense
240 aggregations (66). We hypothesize that estrogen has a direct effect on the endothelium, altering
241 gene expression programs (67) that increase the risk of thrombosis.
242

243 Given what is known about estrogen signaling and our data, we believe that induction of
244 thrombosis is preceded by alteration of transcription or cytoplasmic signaling in endothelial cells.
245 We initially thought it would be easy to determine the first step through ablation of known
246 receptors. However, through knockout and overexpression studies, we found that this effect is not
247 mediated through canonical estrogen NHR or the known G-protein receptor. Despite these
248 paradoxical findings, our data indicate that zebrafish thrombosis is a specific effect of estrogen,
249 which does not occur with other steroid hormones and which is partially blocked by the estrogen
250 antagonist fulvestrant. Finally, there is precedence for alternative targets or receptors. In elegant
251 studies, Kelly and colleagues have clearly demonstrated the existence of a novel estrogen-
252 responsive G-protein receptor, although the gene itself remains undiscovered (18). However, our
253 data with STX suggest this is not our target. There is also evidence for other targets, including ion
254 channels (10, 68). Finally, a recent zebrafish report also discovered that E2 promotes habituation
255 learning through a novel target (19). It is tempting to speculate that estrogen-induced thrombosis
256 may be mediated through one of these targets.
257
258 Surprisingly, estrogen-induced thrombosis persisted despite treatment with potent anticoagulants,
259 as well as loss of common pathway procoagulant factors. We have previously shown that all of
260 these medications and mutations completely block thrombosis in response to endothelial injury
261 (34, 35, 38, 39). Similarly, in our companion drug-screening study, standard anticoagulants had
262 little effect on estrogen-induced thrombosis yet effectively reduced spontaneous thrombosis driven
263 by PC deficiency (66). These data indicate that estrogen-induced thrombi are not solely composed
264 of fibrin secondary to thrombin-mediated cleavage of fibrinogen. However, the results of the a-
265 chain knockout prove that the thrombi are indeed dependent on circulating fibrinogen. Thus, these

266 results are not a fluorescence artifact, since it is known that ablation of *fga* results in absence of
267 fibrinogen (36, 50), and our GFP tag is on the β-chain.
268
269 Interestingly, we found that estrogen-induced thrombosis depends on the TF paralogs, primarily
270 *f3b*, and synergy when combined with *f3a*. This result contrasts with our previous study using a
271 laser-endothelial injury model, where *f3b* drives arterial occlusion and *f3a* was primary in the
272 venous system (52). However, that study also showed concordance with estrogen-induced
273 thrombosis in that *f3b* was more effective for spontaneous venous thrombosis, which is known to
274 be a consequence of antithrombin (*at3*) deficiency[34], and was also synergistic with *f3a* (52). Laser-
275 injury-induced thrombosis represents an acute hemostatic response, whereby damaged endothelial
276 cells lead to vessel occlusion due to rapid recruitment of thrombocytes and formation of fibrin, in
277 the arterial and venous systems, respectively. By contrast, estrogen-induced and spontaneous
278 thromboses develop over hours to days, are independent of thrombocytes, and occur across and
279 exclusively in the venous circulation, reflecting a chronic, hypercoagulable state rather than a site-
280 specific injury. The data suggest the possibility of a resident *f3b* pool in the venous circulation that
281 comes into play upon estrogen treatment without vascular injury. However, elevated levels of
282 estrogen are known to affect inflammation (69, 70). Thus, an alternative is that TF is known to not
283 be restricted to the endothelium, and monocytes, macrophages, and neutrophils also express TF
284 under inflammatory conditions (71).
285
286 The next question we plan to address in future studies is the structure of these thrombi. Our data
287 suggest several possibilities. The anticoagulants do inhibit thrombosis to a degree, so fibrin may
288 be a partial component. Additionally, we found polyhedrocytes, which are known to form upon

289 clot contraction (46). However, complete loss of the *f2* and *f10* genes should block all fibrin
290 formation. Thus, there could be an alternative means of generating fibrin independent of thrombin,
291 but this seems unlikely as there is no evidence for such a protease. A more likely hypothesis is that
292 estrogen-induced thrombi are composed of crosslinked fibrinogen. It has previously been shown
293 that non-factor XIII transglutaminases have this capability *ex vivo* (72). More recently, tissue
294 transglutaminase-2 (TGM2) was shown to crosslink fibrin(ogen) in the setting of experimental
295 liver fibrosis (73). Most intriguingly, injection of a Tgm2 fluorescent competitive substrate into
296 zebrafish larvae yielded a labeling pattern (74) that bears a striking similarity to what we observe
297 for estrogen-induced thrombosis. Tgm2 activity in zebrafish is primarily composed of two
298 ohnologs (*tgm2a* and *b*), which were shown to be expressed during the larval period (1-5 dpf)(74).
299
300 We have found that estrogen-induced thrombosis in zebrafish shares many features consistent with
301 human disease. Additionally, our findings reveal several unexpected aspects, including the
302 involvement of a novel estrogen target/receptor, a connection with TF but not thrombin activity,
303 and evidence of fibrin(ogen) crosslinking. Future studies could develop novel therapeutic targets
304 as well as predict individuals at the highest risk for thrombosis.

305 # Methods

306 ***Sex as a biological variable***

307 All experiments were conducted using zebrafish embryos and larvae within the first 5 dpf. Since
308 gonad differentiation in zebrafish begins after 10 dpf, sex is not a biological variable (75).

309

310 ***Zebrafish***

311 Zebrafish were maintained on a hybrid background of wild-type strains (ABxTL) to minimize
312 strain-specific effects and enhance fecundity. Fish were examined at various developmental stages:
313 embryo (0-2 days post-fertilization, dpf), larvae (3-29 dpf), juvenile (30-89 dpf), and adult (≥90
314 dpf) and housed at 28.5°C, with a 14-hour light/10-hour dark cycle. All procedures were approved
315 by the University of Michigan Animal Care and Use Committee. Previously described transgenic
316 and mutant lines include, *fgb-egfp* (labels fibrin(ogen) with green fluorescence)(76), prothrombin
317 (*f2*)(39), factor X (*f10*)(35), *f3* (52), fibrinogen a-chain (*fga*)(36), *gper1*(60), *flk-mcherry* (red
318 endothelium)(77), *ere-gfp* (estrogen response element reporter)(41), *moonshine* (*mon*^{tg234}, absence
319 of erythrocytes)(78), and *cd41-egfp* (79). Nearly all experiments were performed in the *fgb-egfp*
320 background.

321

322 ***Small molecule treatments***

323 Chemicals were purchased from Sigma-Aldrich, dissolved in DMSO and then in E3 embryo buffer,
324 followed by submersion of larvae in 2 ml E3 embryo buffer (Figure 1A). Final DMSO
325 concentrations were always less than 2%. Larvae were treated at 3-5 dpf for 5-48 hours. Warfarin
326 (50 µg/ml, Sigma-Aldrich) was initiated at 3 dpf and then followed until 5 dpf. Warfarin treatment
327 was alternatively 10 µg/ml from 2 to 5 dpf, with mestranol (25 µM) added at 4 dpf to initiate

328 thrombosis. Separate co-treatments of E2 (50 μM) with fulvestrant (50 μM), dabigatran etexilate
329 (50 μM), or rivoraxaban (250 μM) were performed at 5 dpf for 5 hours. In addition, co-treatment
330 of mestranol (2.5 μM) and fulvestrant (25 μM) was at 3 dpf for 48 hours.
331
332 ***Imaging and quantification of thrombosis***
333 After treatment, zebrafish larvae were anesthetized in tricaine and embedded in 0.8% low-melting
334 point agarose on glass cover slips and visualized on an inverted microscope (Olympus IX71, 20x
335 objective). For all experiments, the observer was blinded to treatment conditions and/or genotype
336 using one of two methods. In the first approach, larvae-embedded slides were labeled and then
337 masked with blank tags by the observer. A second investigator, blinded to the sample conditions,
338 randomized and relabeled the slides in the absence of the observer. In the second method, images
339 were obtained, saved with original filenames, then copied and renamed using randomly generated
340 identifiers (sampling without replacement). In both methods, the key linking original and
341 randomized identifiers was stored separately and accessed only after analysis was completed. In
342 evaluating the thrombosis levels, a semi-quantitative grade was assigned based on the fluorescence
343 intensity in the PCV. Grade 0 indicated no fluorescence, grade 1, sparse puncta, prominent
344 accumulation in grade 2, and grade 3 exhibited dense, nearly complete coverage PCV (Figure 1B).
345 Mutant larvae were recovered from agarose after evaluation and genotyped if needed. Confocal
346 images were acquired by a Nikon A1 high sensitivity confocal microscope. Fluorescence intensity
347 was measured with ImageJ to calculate CTCF as described(34). Concentration-response curves
348 were generated based on both the ordinal thrombosis grading system and the CTCF quantification
349 approach (66). Briefly, thrombosis values from each tested concentration were plotted on a log10-

350 transformed concentration scale using a four-parameter nonlinear regression model (log[agonist]
351 vs. response) in GraphPad Prism (v9.1.0), then normalized to a 0-100% scale.
352
353 ***Measurement of plasma estrogen***
354 After treatment, larvae were washed three times in E3 embryo buffer for 10 minutes, anesthetized,
355 then individually bled in 5 µL of 4% sodium citrate diluted 1:6 in Tyrode's buffer (80), with an
356 estimated whole blood yield of 50 nL and thus 1:100 dilution. Ten larvae were pooled (50 µL),
357 centrifuged at 500g for 10 minutes, and 30 µL supernatant was collected. This was diluted to 0.1
358 mL and mixed with 0.1-0.2 mL water and deuterium-labeled internal standards in 0.1 mL of 40%
359 aqueous methanol. This mixture was applied to a supported liquid extraction cartridge (Isolute,
360 Biotage) and analyzed by mass spectrometry as previously described(81), except that only the
361 1.50-2.65 min window from the first dimension chromatography was passed to the resolving
362 column.
363
364 ***Scanning electron microscopy (SEM)***
365 After treatment with E2, larvae were immobilized using tricaine anesthesia and euthanized on ice.
366 For SEM analysis, sagittal cuts were made in the larvae to open the PCV, rinsed in 50 mM sodium
367 cacodylate buffer (pH 7.5) with 150 mM NaCl, and fixed in 2% glutaraldehyde. Samples were
368 rinsed three times with the cacodylate buffer for 5 minutes and dehydrated in a series of increasing
369 ethanol concentrations, immersed in hexamethyldisilazane, and dried overnight. A thin coating of
370 gold-palladium was layered over the samples using a sputter coater (Polaron e5100, Quorum
371 Technologies). Micrographs were captured using a Quanta 250 FEG scanning electron microscope
372 (ThermoFisher Scientific).

373

374 ***CRISPR-mediated genome editing***

375 We used CRISPR/Cas9 and designed single guide RNAs (sgRNAs) to target upstream and
376 downstream exons, thereby deleting nearly the entire locus of each *esr* gene (Table 1,
377 Supplemental Figure 1) as previously described (52, 82). sgRNAs were complexed with Cas9
378 protein and injected into one-cell embryos. The *esr1* and *esr2a* genes are tightly linked, therefore
379 *esr1* was targeted first, followed by *esr2a* once the former line had been established. Once the
380 *esr1;esr2a* double mutants were produced, they were crossed to *esr2b* mutants to produce triple
381 heterozygotes. *esr1;esr2a;esr2b* triple heterozygotes were incrossed to produce triple homozygous
382 mutant larvae. Genotypes were confirmed using PCR primers (Table 2) and Sanger sequencing.
383 sgRNAs were also designed to create a large deletion that spans the tandem *f7l* and *f7* loci (factors
384 VII-like and VII, respectively), from exon 1 of *f7l* to exon 8 of *f7*, producing a double knockout.

385

386 ***Transgene expression***

387 The *esr1* overexpression plasmid (p*hs-esr1*-Y549S) was constructed by inserting the *esr1*-Y549S
388 cDNA into a vector under control of the heat shock promoter(83) downstream of *mcherry* and a
389 p2A sequence, all flanked by Tol2 repeats. 20-25 picograms plasmid was injected into *fgb-egfp*
390 and *ere-gfp* one-cell stage embryos. At 3 dpf, larvae were incubated at 35ºC and evaluated for
391 thrombosis.

392

393 ***Statistical analysis***

394 Statistical analyses were performed using two-tailed Fisher exact, Student t-test and Spearman's
395 rank correlation test. Charts were generated using GraphPad Prism (v9.1.0, San Diego, CA, USA)
396 and R (v4.3.3).
397
398 ***Study approval***
399 All experiments were conducted in accordance with guidelines approved by the Institutional
400 Animal Care and Use Committee (IACUC) of the University of Michigan (Protocol Numbers:
401 PRO00010679 & PRO00012352).
402
403 ***Data availability***
404 Data for all graphs are provided in the Supporting Data Values supplemental file.

Authorship contributions

X.Y. and M.Y. designed and performed research, analyzed data, and wrote the manuscript. X.Y. and J.A.S. conceived of the project, and this was used to decide the order of co-authorship. Q.Y.Z., S.M.E., J.K.L., H.S. performed research and analyzed data. A.C.F., C.N., S.C. performed research, W.G., J.W.W., R.A. designed and supervised research and analyzed data, J.A.S. designed, performed, and supervised research, analyzed data, and wrote the manuscript. All authors reviewed the manuscript.

Acknowledgements

The authors thank Martin Kelly for helpful discussions and providing STX compound, and Dan Gorelick for providing the *ere-gfp* line. This work was supported by National Institutes of Health grants R01 ES032255, R35 HL150784 (J.A.S.), R01 DK090311, R24 OD035402 (W.G.), and R01 HL148227, P01 HL146373, R01 HL148014, R01 HL159256 (J.W.W.), and a pilot grant from the University of Michigan Frankel Cardiovascular Center M-BRISC program. J.A.S. is the Henry and Mala Dorfman Family Professor of Pediatric Hematology/Oncology.

422 # References

423 1. CDC. Venous Thromboembolism (Blood Clots). https://www.cdc.gov/blood-clots/about/.
424 Accessed October 24, 2025.
425 2. LaVasseur C, et al. Hormonal therapies and venous thrombosis: Considerations for
426 prevention and management. *Res Pract Thromb Haemost.* 2022;6(6):e12763.
427 3. Lutsey PL, and Zakai NA. Epidemiology and prevention of venous thromboembolism. *Nat*
428 *Rev Cardiol.* 2023;20(4):248-62.
429 4. Rosendaal F, et al. Female hormones and thrombosis. *Arteriosclerosis, thrombosis, and*
430 *vascular biology.* 2002;22(2):201-10.
431 5. Daly E, et al. Risk of venous thromboembolism in users of hormone replacement therapy.
432 *The Lancet.* 1996;348(9033):977-80.
433 6. Mammen EF. Oral contraceptives and blood coagulation: a critical review. *American*
434 *Journal of Obstetrics and Gynecology.* 1982;142(6):781-90.
435 7. Cushman M, et al. Estrogen plus progestin and risk of venous thrombosis. *Jama.*
436 2004;292(13):1573-80.
437 8. Abou-Ismail MY, et al. Estrogen and thrombosis: a bench to bedside review. *Thrombosis*
438 *research.* 2020;192:40-51.
439 9. Barton M, et al. Twenty years of the G protein-coupled estrogen receptor GPER: Historical
440 and personal perspectives. *The Journal of steroid biochemistry and molecular biology.*
441 2018;176:4-15.
442 10. Treviño LS, and Gorelick DA. The interface of nuclear and membrane steroid signaling.
443 *Endocrinology.* 2021;162(8):bqab107.
444 11. Beri R, et al. Estrogenic and progestational activity of 7α-methyl-19-nortestosterone, a
445 synthetic androgen. *The Journal of steroid biochemistry and molecular biology.*
446 1998;67(3):275-83.
447 12. Kuhl H. Comparative pharmacology of newer progestogens. *Drugs.* 1996;51:188-215.
448 13. Fuentes N, and Silveyra P. Estrogen receptor signaling mechanisms. *Advances in protein*
449 *chemistry and structural biology.* 2019;116:135-70.
450 14. Menuet A, et al. Analysis of the estrogen regulation of the zebrafish estrogen receptor (ER)
451 reveals distinct effects of ERalpha, ERbeta1 and ERbeta2. *Journal of molecular*
452 *endocrinology.* 2004;32(3):975-86.
453 15. Tingaud-Sequeira A, et al. Expression patterns of three estrogen receptor genes during
454 zebrafish (Danio rerio) development: evidence for high expression in neuromasts. *Gene*
455 *Expression Patterns.* 2004;4(5):561-8.
456 16. Kuntz MA, and Shapiro DJ. Dimerizing the estrogen receptor DNA binding domain
457 enhances binding to estrogen response elements. *Journal of Biological Chemistry.*
458 1997;272(44):27949-56.
459 17. Prossnitz ER, and Barton M. The G protein-coupled oestrogen receptor GPER in health
460 and disease: an update. *Nature Reviews Endocrinology.* 2023;19(7):407-24.
461 18. Qiu J, et al. A G-protein-coupled estrogen receptor is involved in hypothalamic control of
462 energy homeostasis. *J Neurosci.* 2006;26(21):5649-55.
463 19. Hsiao A, et al. Estradiol Promotes Habituation Learning via an Unidentified Target,
464 Bypassing the Suppressive Effects of Established ERs. *Endocrinology.* 2025;166(8).
465 20. Lu CL, and Herndon C. New roles for neuronal estrogen receptors. *Neurogastroenterology*
466 *& Motility.* 2017;29(7):e13121.

21. Yoh K, et al. Roles of estrogen, estrogen receptors, and estrogen-related receptors in skeletal muscle: regulation of mitochondrial function. *International journal of molecular sciences.* 2023;24(3):1853.
22. Schmid S, and Fent K. 17β-Estradiol and the glucocorticoid clobetasol propionate affect the blood coagulation cascade in zebrafish. *Environmental Pollution.* 2020;259:113808.
23. Cosman F, et al. Short-term effects of estrogen, tamoxifen and raloxifene on hemostasis: a randomized-controlled study and review of the literature. *Thrombosis research.* 2005;116(1):1-13.
24. Cleuren AC, et al. 17α-Ethinylestradiol rapidly alters transcript levels of murine coagulation genes via estrogen receptor α. *J Thromb Haemost.* 2010;8(8):1838-46.
25. Kemmeren JM, et al. Effect of second-and third-generation oral contraceptives on the protein C system in the absence or presence of the factor VLeiden mutation: a randomized trial. *Blood.* 2004;103(3):927-33.
26. Tans G, et al. *A randomized cross-over study on the effects of levonorgestrel- and desogestrel-containing oral contraceptives on the anticoagulant pathways.* 2000.
27. Kim CS, et al. Estrogen activates endothelial exocytosis. *Biochem Biophys Res Commun.* 2021;558:29-35.
28. Bouck EG, et al. High risk oral contraceptive hormones do not directly enhance endothelial cell procoagulant activity in vitro. *PLoS One.* 2023;18(4):e0284333.
29. Cleuren AC, et al. Long-term estrogen treatment of mice with a prothrombotic phenotype induces sustained increases in thrombin generation without affecting tissue fibrin deposition. *J Thromb Haemost.* 2012;10(11):2392-4.
30. Cleuren AC, et al. Short-term ethinyl estradiol treatment suppresses inferior caval vein thrombosis in obese mice. *Thromb Haemost.* 2009;102(5):993-1000.
31. Weyand AC, and Shavit JA. Zebrafish as a model system for the study of hemostasis and thrombosis. *Curr Opin Hematol.* 2014;21(5):418-22.
32. Kretz CA, et al. Modeling Disorders of Blood Coagulation in the Zebrafish. *Curr Pathobiol Rep.* 2015;3(2):155-61.
33. Jagadeeswaran P, et al. Animal Models of Thrombosis From Zebrafish to Nonhuman Primates: Use in the Elucidation of New Pathologic Pathways and the Development of Antithrombotic Drugs. *Circ Res.* 2016;118(9):1363-79.
34. Liu Y, et al. Targeted mutagenesis of zebrafish antithrombin III triggers disseminated intravascular coagulation and thrombosis, revealing insight into function. *Blood.* 2014;124(1):142-50.
35. Hu Z, et al. Genome editing of factor X in zebrafish reveals unexpected tolerance of severe defects in the common pathway. *Blood.* 2017;130(5):666-76.
36. Hu Z, et al. Loss of fibrinogen in zebrafish results in an asymptomatic embryonic hemostatic defect and synthetic lethality with thrombocytopenia. *J Thromb Haemost.* 2019;17(4):607-17.
37. Weyand AC, et al. Analysis of factor V in zebrafish demonstrates minimal levels needed for early hemostasis. *Blood Adv.* 2019;3(11):1670-80.
38. Raghunath A, et al. Fishing for answers to hemostatic and thrombotic disease: Genome editing in zebrafish. *Res Pract Thromb Haemost.* 2022;6(5):e12759.
39. Grzegorski SJ, et al. Disruption of the kringle 1 domain of prothrombin leads to late onset mortality in zebrafish. *Sci Rep.* 2020;10(1):4049.

512 40. Schaaf MJ. Nuclear receptor research in zebrafish. *Journal of molecular endocrinology.*
513 2017;59(1):R65-R76.
514 41. Gorelick DA, and Halpern ME. Visualization of estrogen receptor transcriptional
515 activation in zebrafish. *Endocrinology.* 2011;152(7):2690-703.
516 42. Romano SN, and Gorelick DA. Crosstalk between nuclear and G protein-coupled estrogen
517 receptors. *Gen Comp Endocrinol.* 2018;261:190-7.
518 43. Walker RF, et al. Association of Testosterone Therapy With Risk of Venous
519 Thromboembolism Among Men With and Without Hypogonadism. *JAMA Internal*
520 *Medicine.* 2020;180(2):190-7.
521 44. Cines DB, et al. Clot contraction: compression of erythrocytes into tightly packed
522 polyhedra and redistribution of platelets and fibrin. *Blood.* 2014;123(10):1596-603.
523 45. Lassila R, and Weisel JW. Role of red blood cells in clinically relevant bleeding tendencies
524 and complications. *J Thromb Haemost.* 2023;21(11):3024-32.
525 46. Griffin MS, et al. Composition of thrombi in zebrafish: similarities and distinctions with
526 mammals. *J Thromb Haemost.* 2024;22(4):1056-68.
527 47. Suh TT, et al. Resolution of spontaneous bleeding events but failure of pregnancy in
528 fibrinogen-deficient mice. *Genes Dev.* 1995;9(16):2020-33.
529 48. Casini A, et al. Heterogeneity of congenital afibrinogenemia, from epidemiology to clinical
530 consequences and management. *Blood Rev.* 2021;48:100793.
531 49. Dobson DA, et al. Regulation of fibrinogen synthesis. *Thromb Res.* 2024;242:109134.
532 50. Fish RJ, et al. Targeted mutation of zebrafish fga models human congenital
533 afibrinogenemia. *Blood.* 2014;123(14):2278-81.
534 51. Zelaya H, et al. Tissue factor at the crossroad of coagulation and cell signaling. *J Thromb*
535 *Haemost.* 2018;16(10):1941-52.
536 52. Grzegorski SJ, et al. Genetic duplication of tissue factor reveals subfunctionalization in
537 venous and arterial hemostasis. *PLoS Genet.* 2022;18(11):e1010534.
538 53. Howe K, et al. The zebrafish reference genome sequence and its relationship to the human
539 genome. *Nature.* 2013;496(7446):498-503.
540 54. Gregory M, et al. Genetic analysis of hemostasis and thrombosis using vascular occlusion.
541 *Blood Cells Mol Dis.* 2002;29(3):286-95.
542 55. Sheehan J, et al. Demonstration of the extrinsic coagulation pathway in teleostei:
543 identification of zebrafish coagulation factor VII. *Proc Natl Acad Sci U S A.*
544 2001;98(15):8768-73.
545 56. Hanumanthaiah R, et al. Comprehensive analysis of blood coagulation pathways in
546 teleostei: evolution of coagulation factor genes and identification of zebrafish factor VIIi.
547 *Blood Cells Mol Dis.* 2002;29(1):57-68.
548 57. Wolford BN, et al. Multipopulation GWAS for venous thromboembolism identifies novel
549 loci followed by experimental validation in zebrafish. *Blood Adv.* 2025;9(19):4850-9.
550 58. Carlson RW. The history and mechanism of action of fulvestrant. *Clin Breast Cancer.*
551 2005;6 Suppl 1:S5-8.
552 59. Lu H, et al. Functional Analysis of Nuclear Estrogen Receptors in Zebrafish Reproduction
553 by Genome Editing Approach. *Endocrinology.* 2017;158(7):2292-308.
554 60. Chaturantabut S, et al. Estrogen Activation of G-Protein-Coupled Estrogen Receptor 1
555 Regulates Phosphoinositide 3-Kinase and mTOR Signaling to Promote Liver Growth in
556 Zebrafish and Proliferation of Human Hepatocytes. *Gastroenterology.* 2019;156(6):1788-
557 804 e13.

558 61. Lee H-J, et al. Neuroprotection against beta-amyloid toxicity by the novel estrogen receptor
559 modulator STX requires convergent signaling pathways. *Frontiers in Molecular*
560 *Neuroscience.* 2025;Volume 18 - 2025.
561 62. Postlethwait JH. The zebrafish genome in context: ohnologs gone missing. *J Exp Zool B*
562 *Mol Dev Evol.* 2007;308(5):563-77.
563 63. Parajes S, et al. Endothelial and non-endothelial responses to estrogen excess during
564 development lead to vascular malformations [preprint]. *bioRxiv.* 2018:320234.
565 64. Mosimann C, et al. Ubiquitous transgene expression and Cre-based recombination driven
566 by the ubiquitin promoter in zebrafish. *Development.* 2011;138(1):169-77.
567 65. Ku CJ, et al. Loss of protein C vs protein S results in discrepant thrombotic phenotypes.
568 *Blood Adv.* 2025;9(3):545-57.
569 66. Yaman M, et al. FDA-approved drug repurposing in zebrafish identifies thyroid hormone
570 and other compounds as potential antithrombotics [preprint]. *bioRxiv.* 2025.
571 67. Cleuren ACA, et al. The in vivo endothelial cell translatome is highly heterogeneous across
572 vascular beds. *Proc Natl Acad Sci U S A.* 2019;116(47):23618-24.
573 68. Kow LM, and Pfaff DW. Rapid estrogen actions on ion channels: A survey in search for
574 mechanisms. *Steroids.* 2016;111:46-53.
575 69. Park M, et al. Macrophages: a double-edged sword in female reproduction and disorders.
576 *Experimental & Molecular Medicine.* 2025;57(2):285-97.
577 70. Novella S, et al. Effects of Estrogen on Vascular Inflammation. *Arteriosclerosis,*
578 *Thrombosis, and Vascular Biology.* 2012;32(8):2035-42.
579 71. Grover SP, and Mackman N. Tissue Factor. *Arteriosclerosis, Thrombosis, and Vascular*
580 *Biology.* 2018;38(4):709-25.
581 72. Murthy SN, and Lorand L. Cross-linked A alpha.gamma chain hybrids serve as unique
582 markers for fibrinogen polymerized by tissue transglutaminase. *Proc Natl Acad Sci U S A.*
583 1990;87(24):9679-82.
584 73. Poole LG, et al. Chronic liver injury drives non-traditional intrahepatic fibrin(ogen)
585 crosslinking via tissue transglutaminase. *J Thromb Haemost.* 2019;17(1):113-25.
586 74. Lisetto M, et al. Biochemical and Functional Characterization of the Three Zebrafish
587 Transglutaminases 2. *Int J Mol Sci.* 2023;24(15).
588 75. King AC, et al. Shedding new light on early sex determination in zebrafish. *Arch Toxicol.*
589 2020;94(12):4143-58.
590 76. Vo AH, et al. Loss of fibrinogen in zebrafish results in symptoms consistent with human
591 hypofibrinogenemia. *PLoS One.* 2013;8(9):e74682.
592 77. Proulx K, et al. Cranial vasculature in zebrafish forms by angioblast cluster-derived
593 angiogenesis. *Developmental biology.* 2010;348(1):34-46.
594 78. Ransom DG, et al. The zebrafish moonshine gene encodes transcriptional intermediary
595 factor 1gamma, an essential regulator of hematopoiesis. *PLoS Biol.* 2004;2(8):E237.
596 79. Lin HF, et al. Analysis of thrombocyte development in CD41-GFP transgenic zebrafish.
597 *Blood.* 2005;106(12):3803-10.
598 80. Rost MS, et al. Nfe2 is dispensable for early but required for adult thrombocyte formation
599 and function in zebrafish. *Blood Adv.* 2018;2(23):3418-27.
600 81. Banker M, et al. Association of Maternal-Neonatal Steroids With Early Pregnancy
601 Endocrine Disrupting Chemicals and Pregnancy Outcomes. *J Clin Endocrinol Metab.*
602 2021;106(3):665-87.

603 82. Raghunath A, et al. Loss of factor VIII in zebrafish rebalances antithrombin deficiency but
604 has a limited bleeding diathesis. *Blood Advances.* 2025;9(13):3136-48.
605 83. Shoji W, and Sato-Maeda M. Application of heat shock promoter in transgenic zebrafish.
606 *Dev Growth Differ.* 2008;50(6):401-6.

607

608

609 **Figures**

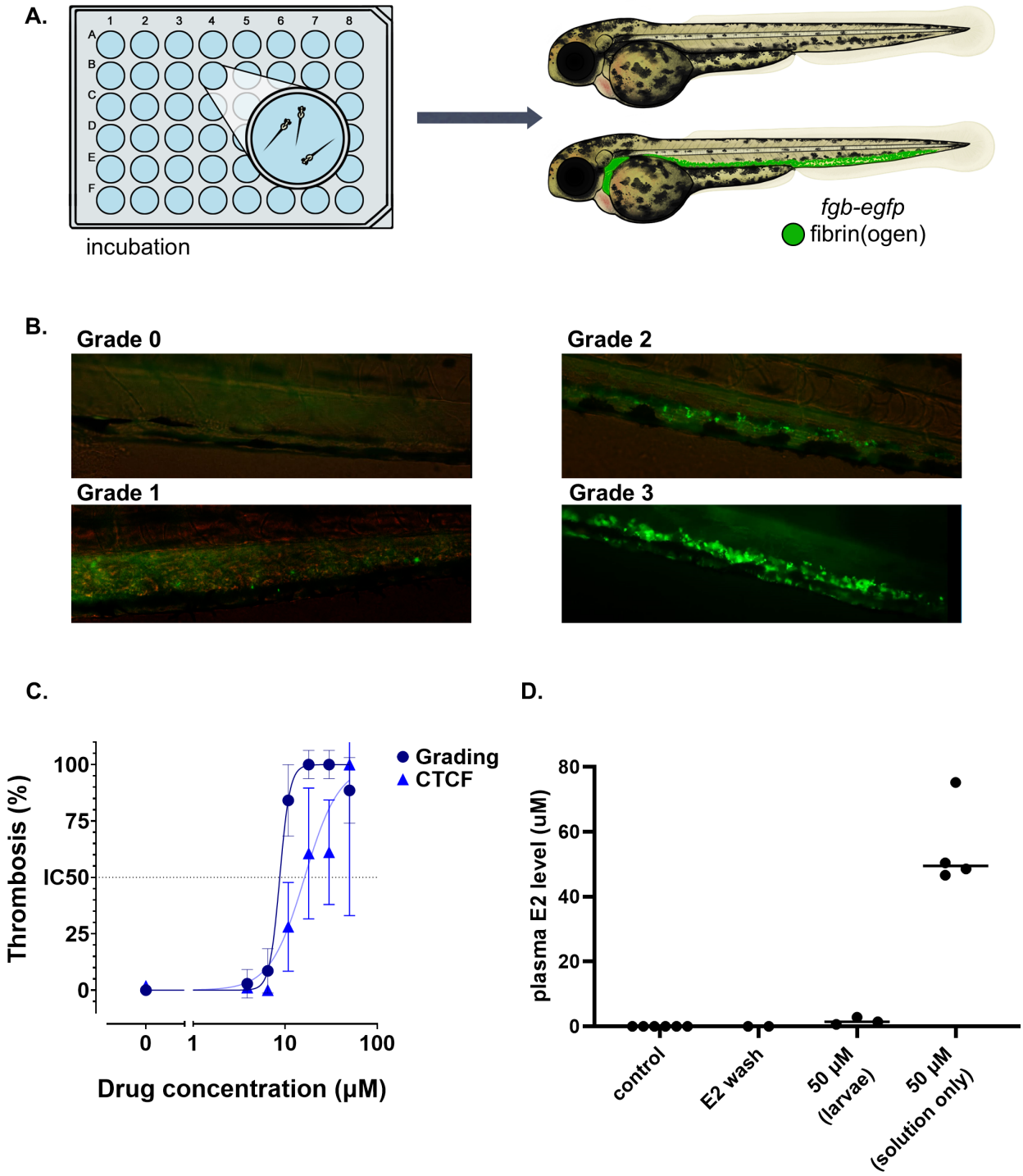

610
611 **Figure 1: Induction and quantification of thrombosis in zebrafish larvae.** (A) Estrogenic
612 compounds were dissolved in DMSO and added to multiwell plates with E3 embryo buffer. *fgb-*

613 *egfp* transgenic larvae, which generate GFP-tagged fibrin(ogen), were added at 3-5 dpf and
614 incubated up to 48 hours. After incubation, larvae were briefly washed with system water and then
615 mounted in 0.8% agarose and evaluated with a compound microscope and 20x objective. After
616 incubation, estrogen-treated fish developed GFP-labeled thrombosis in the PCV, indicating
617 fibrin(ogen) deposition, which was graded. (B) Representative images for the semi-quantitative
618 grading system. Scoring was always performed by an observer blinded to condition and/or
619 genotype as follows: Grade 0: no fluorescence accumulation. Grade 1: small sporadic fluorescent
620 puncta seen scattered in the PCV. Grade 2: continuous fluorescence spreading across the PCV.
621 Grade 3: strong fluorescence visualized across the PCV. (C) Quantification of fluorescence by
622 CTCF in comparison with semi-quantitative grading. Each point represents the mean values from
623 n=9-12 larvae, with error bars showing 95% confidence intervals. (D) Quantification of plasma
624 levels of 17β-estradiol (E2) after treatment in 25 and 50 μM E2 and controls. Larvae were bled
625 into buffer and then pooled for mass spectrometry. "E2 wash" indicates larvae washed with 50 μM
626 E2 and then system water, without prior incubation in E2. "50 μM (solution only)" is quantification
627 of the E2 containing buffer without larvae. Each point represents a pool of 10 larvae.

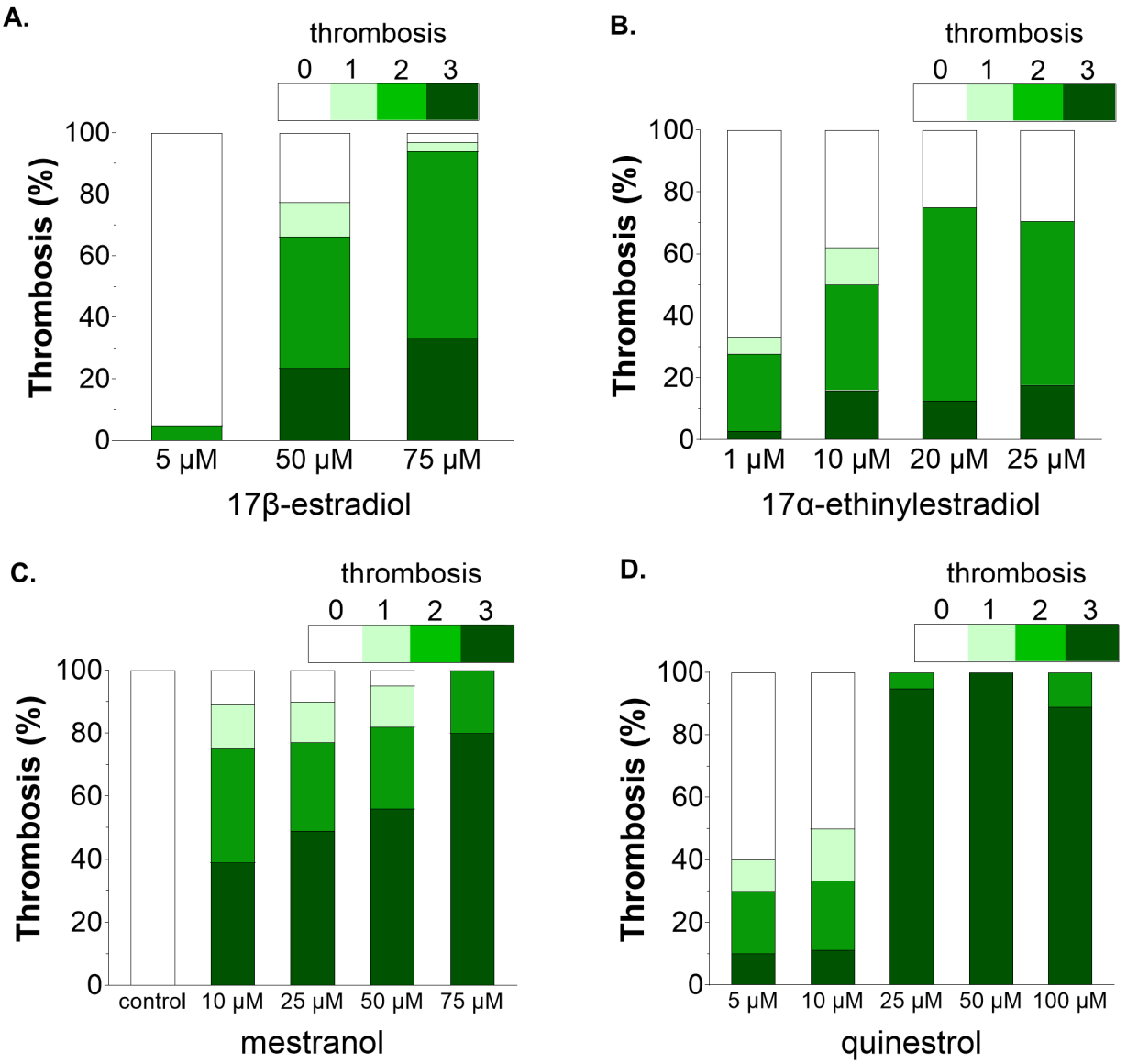

628

629 **Figure 2: Estrogen analogs induce dose-dependent *in vivo* thrombosis.** Dose-dependent
630 increases in thrombosis were observed with multiple estrogens. (A) 17β-estradiol (E2) treatment
631 for 5 hours at 5 dpf. n=41, 234, 33. (B) 17α-ethinylestradiol (EE2) treatment for 24 hours at 4 dpf.
632 n=36, 50, 8, 17. (C) Mestranol treatment for 24 hours at 4 dpf. n=24, 38, 39, 39, 20. (D) Quinestrol
633 treatment for 24 hours at 4 dpf. n=10-19 in each group. All incubations were performed in the *fgb-*
634 *egfp* transgenic background and data collected by an observer blinded to condition.

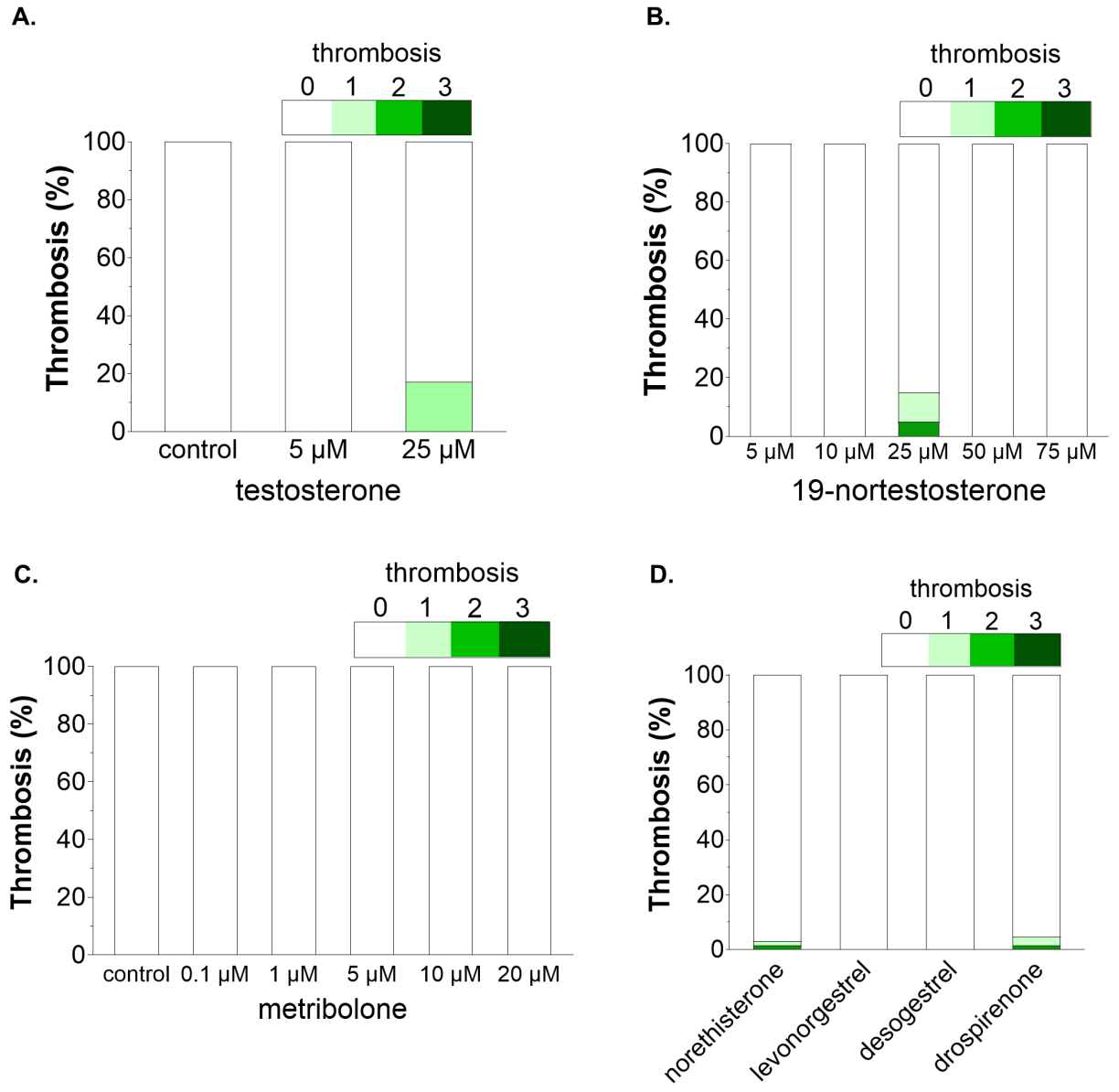

Figure 3: Testosterone derivatives and progestins do not cause thrombosis. (A) Testosterone incubations were performed for 24 hours starting at 4 dpf. (B) 19-nortestosterone incubations were for 48 hours starting at 3 dpf. (C) Metribolone incubations were 24 hours starting at 4 dpf. n=10-30 for each testosterone derivative concentration. (D) Multiple progestins were evaluated at the maximum tolerated dose for 5 hours on 5 dpf. Norethisterone 10 μM, levonogestrel 25 μM, desogestrel 1 μM, drospirenone 25 μM. n=30-65 for each group. All data were collected in the *fgb-egfp* transgenic background by an observer blinded to condition.

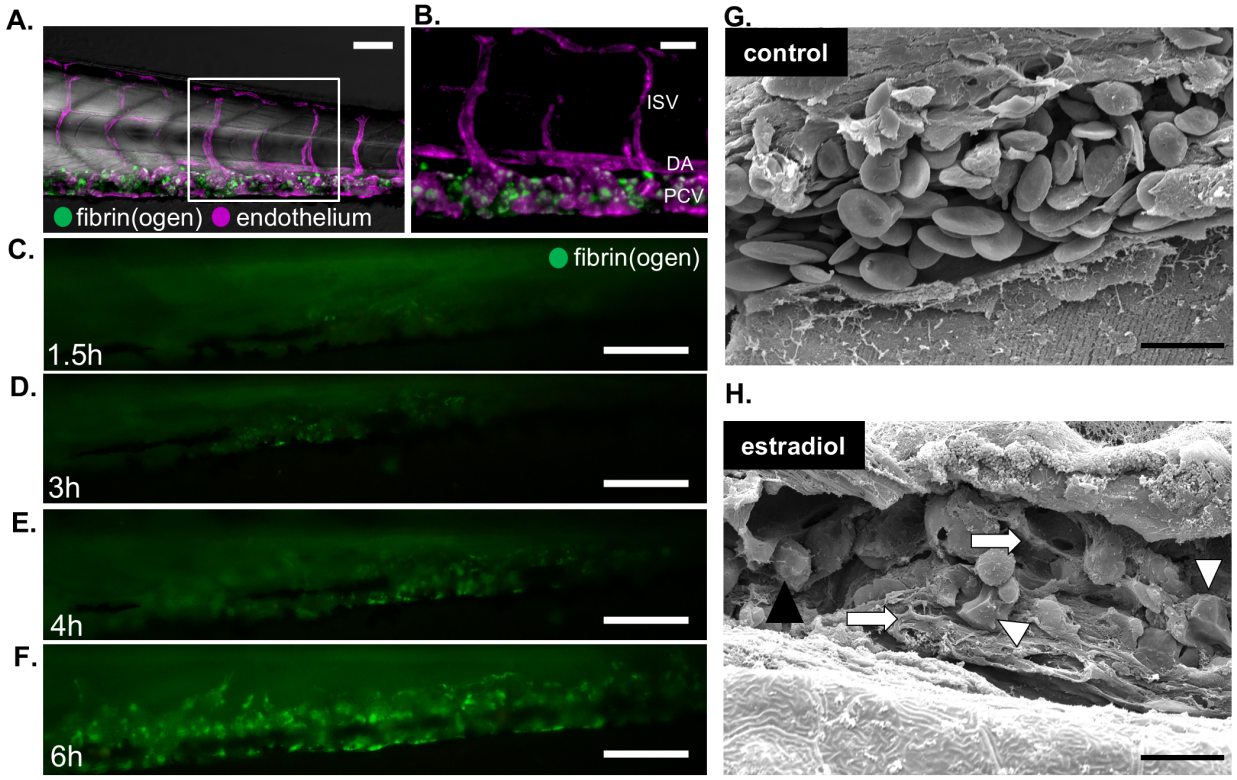

Figure 4: Static and time-lapse imaging of estrogen-induced thrombosis. (A-B) Fish larvae were from an *fgb-egfp*;*flk-mcherry* hybrid background, false colored to represent thrombi in green and endothelial cells in magenta. Confocal microscopy demonstrates that the GFP-labeled thrombi were contained within the PCV, and not the dorsal aorta (DA) or intersegment vessels (ISV). Scale bars, (A) 100 µm, (B) 20 µm. (C-F) Compound microscopy time-lapse images of thrombosis formation over 6 hours reveal initiation simultaneously along the PCV, rather than from a single location. Scale bars, 100 µm. (G-H) Scanning electron microscopic images comparing the PCV of a DMSO (control) treated fish (G) and a grade 2 larvae treated with E2 (H). In the control group, erythrocytes exhibit typical flat and oval morphology. In the treated larva, scattered fibers that may be fibrin(ogen) are seen attached to erythrocytes (arrows). Polyhedrocytes (arrowheads) are observed, suggestive of clot contraction. Scale bars in (G-H), 10 µm.

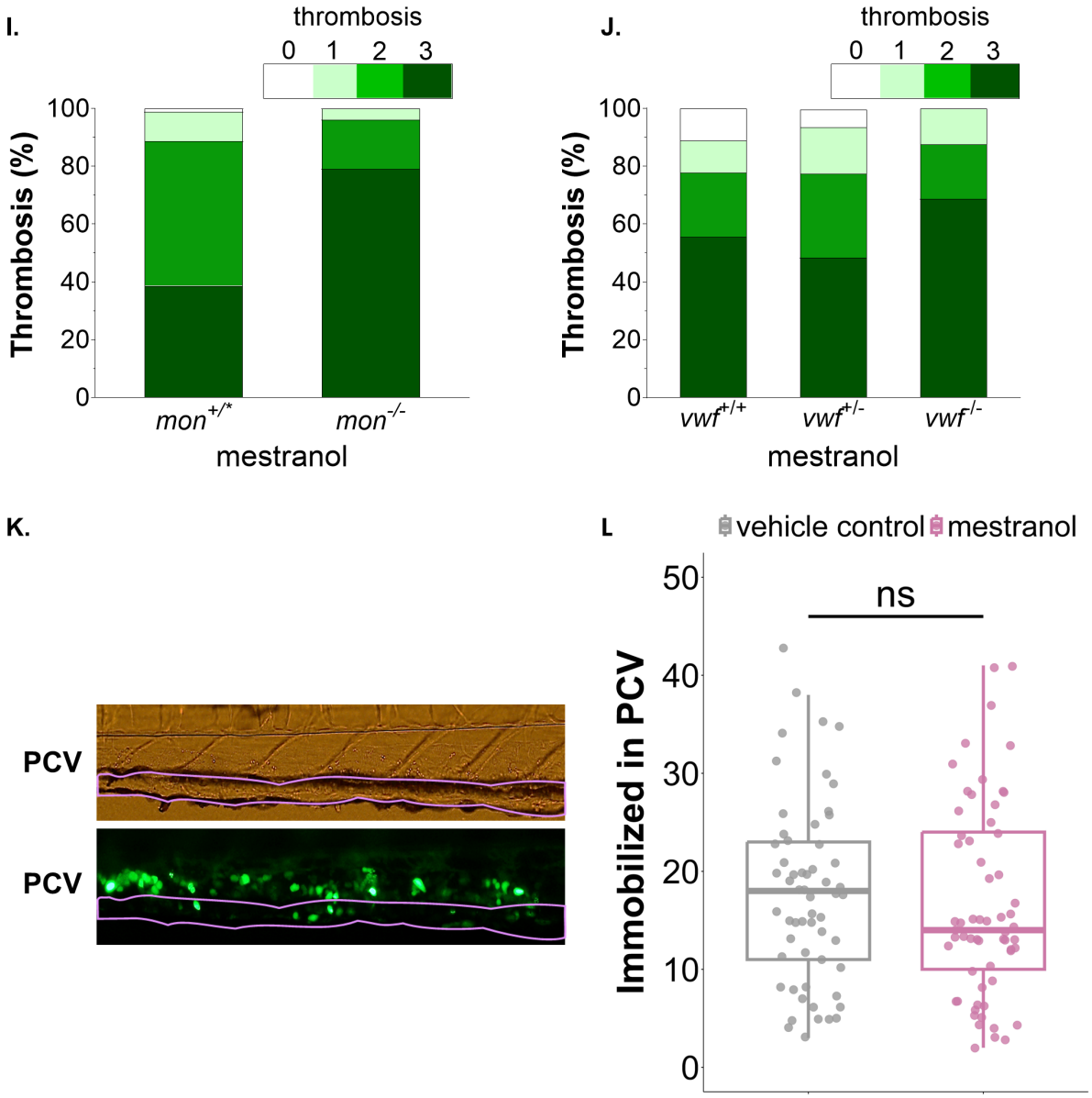

Figure 4 (cont'd). (I-J) 48 hour mestranol treatments in offspring from *mon*$^{+/-}$ incrosses (n=88 in *mon*$^{+/*}$, mix of wild-type and heterozygotes, 24 in *mon*$^{-/-}$; 3→5 dpf with 5 µM mestranol) and *vwf*$^{+/-}$ incrosses (n=18, 31, 16; 2→4 dpf with 25 µM mestranol). $p < 0.005$ between *mon* groups, and no statistical significance in *vwf* using Fisher exact test. (K-L) Thrombocyte counting across larvae treated with vehicle control (DMSO) and mestranol (25 µM) for 24 hours and observed at 5 dpf (n=58, 61). (K) A thrombocyte reporter line (*cd41-egfp*) was utilized and the PCV regions (magenta outline) were selected based on brightfield and fluorescence images. (L) Immobilized thrombocytes were counted in the outlined PCV regions, and box-and-whisker plots are shown (vehicle control: box=11-23, median=18, whiskers=3-38, outlier=43; mestranol: box=10-24, median=14, whiskers=2-41, no outliers). No significant difference (ns) was detected by Student t-test. Except for K and L, all data were collected in the *fgb-egfp* transgenic background. All data were collected by an observer blinded to condition.

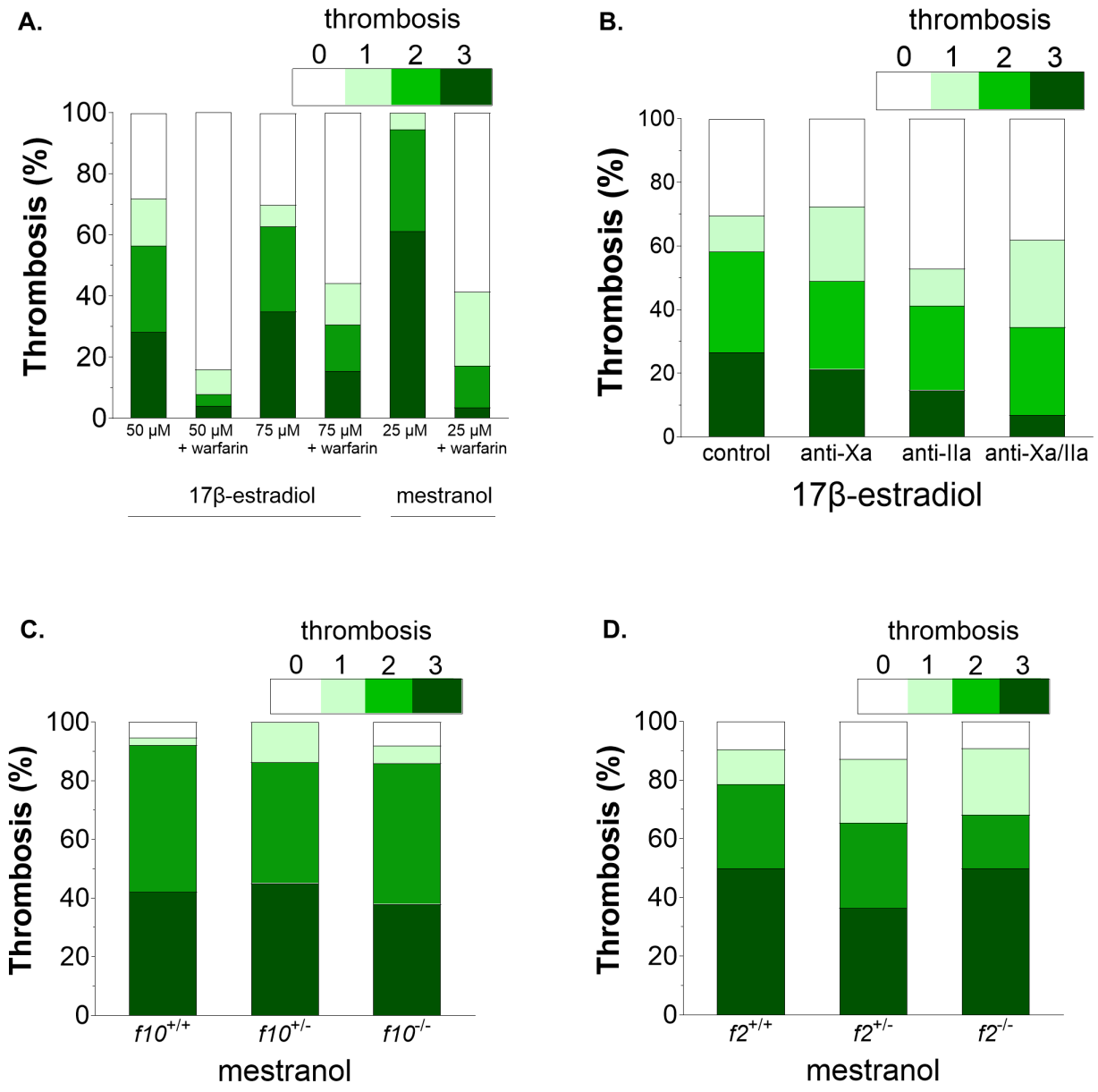

Figure 5: Estrogen-induced thrombi are dependent on fibrin(ogen), but not the canonical coagulation cascade. (A) Larvae were pretreated with warfarin, followed by estrogens. In the first group, warfarin (50 µg/ml) was initiated at 3 dpf, followed by E2 for 5 hours at 5 dpf. The mestranol-exposed larvae were pretreated with warfarin (10 µg/ml) at 2 dpf, followed by 25 µM mestranol for 24 hours starting at 4 dpf. n= 39, 25, 43, 52, 18, and 29. p=0.0001 for 50 µM E2 treatment, p=0.002 for 75 µM E2, p<0.0001 for mestranol. (B) Larvae were co-treated with E2 and rivaroxaban (anti-Xa) or dabigatran etexilate (anti-IIa) at 250 and 50 µM, respectively, for 5 hours at 5 dpf. n=103, 74, 50, and 51. p=0.03 (anti-Xa), 0.03 (anti-IIa), 0.001 (combination). (C-D) 48 hours of mestranol treatments in offspring from, *f10*$^{+/-}$ incrosses (n=38, 51, and 50; 3→5 dpf with 5 µM mestranol), and *f2*$^{+/-}$ incrosses (n=42, 55, 22, 2→4 dpf with 25 µM mestranol). No statistically significant differences were observed.

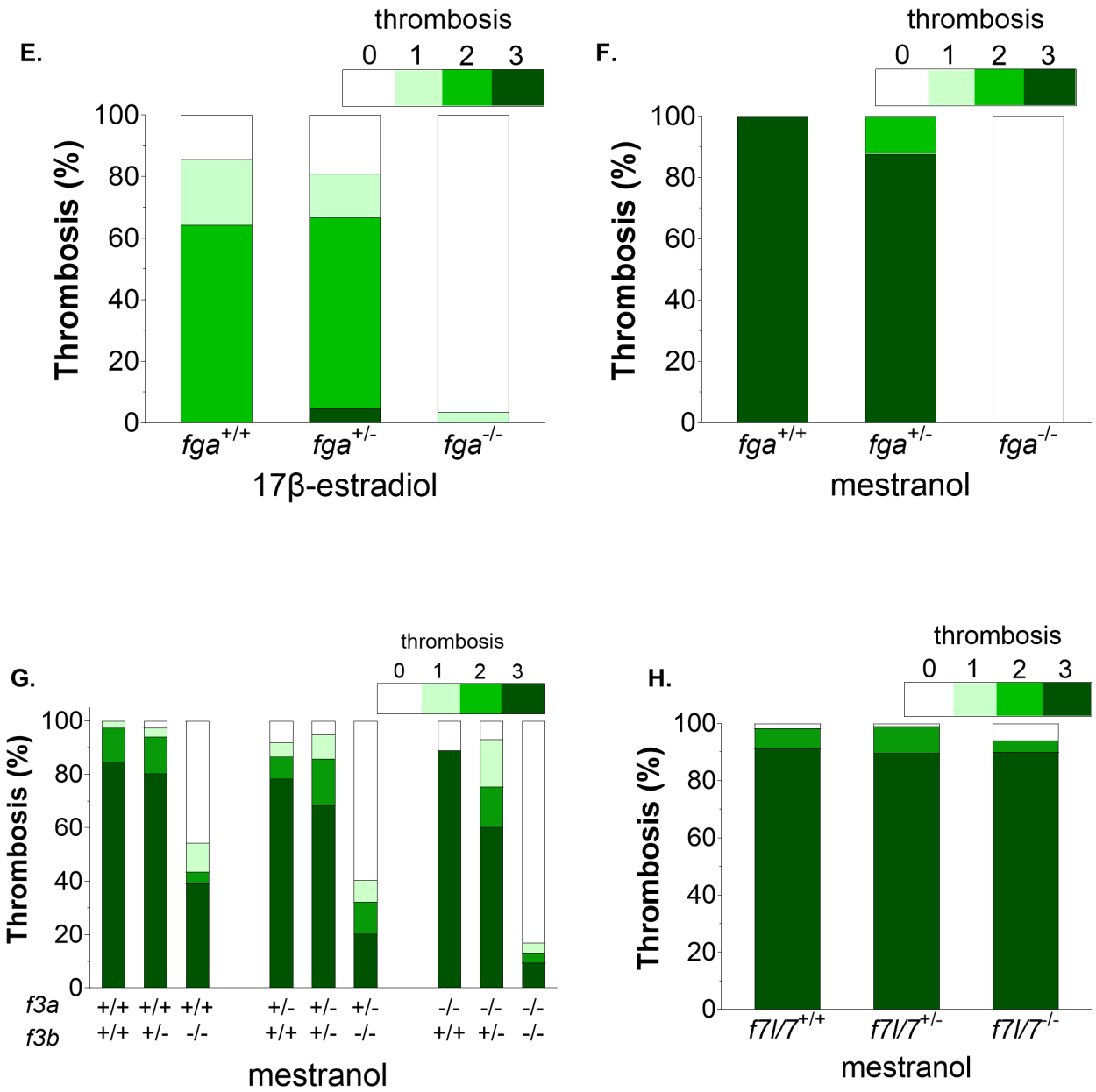

Figure 5 (cont'd). (E) Offspring from *fga*$^{+/-}$ incrosses were treated with 50 µM E2 (n=14, 42, and 28 at 5 dpf for 5 hours) or (F) 25 µM mestranol (n= 18, 41, and 27 at 3 dpf for 48 hours), resulting in essentially no thrombi. p<0.0001 for both groups. (G) 25 µM mestranol treatment in *f3a*$^{+/-}$;*f3b*$^{+/-}$ incrosses (n=39, 116, 92 for the *f3a*$^{+/+}$ strata; 37, 154, 99 for the *f3a*$^{+/-}$ strata; 27, 73, 53 for the *f3a*$^{-/-}$ strata). p<0.0001 for each comparison of *f3b* genotypes within separate *f3a* strata, and p=0.0002 for comparison of the *f3a* genotype within the *f3b*$^{-/-}$ genotype group, while there was no significant difference for comparison of *f3a* to the other *f3b* genotype groups. (H) Mestranol treatment in offspring from *f7l/7*$^{+/-}$ incrosses treated with 25 µM mestranol (n=58, 106, and 51; 3→5 dpf for 48 hours) with no significant differences based on *f7l/7* genotype. All data were collected in the *fgb-egfp* transgenic background by an observer blinded to condition and/or genotype. Fisher exact test was applied for all statistical comparisons.

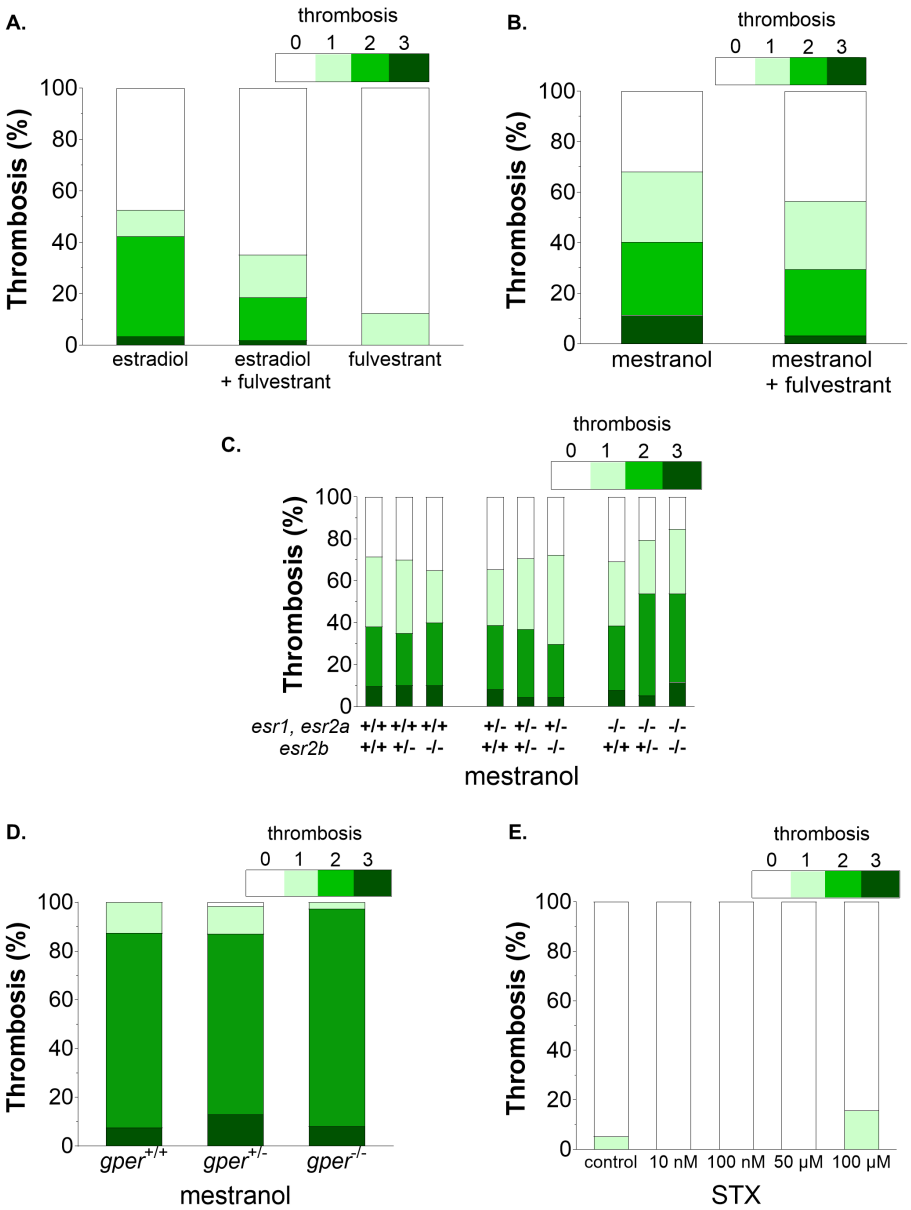

Figure 6: Estrogen-induced thrombosis appears to be mediated through a non-canonical estrogen target. (A) Co-treatment of E2 (50 µM) and fulvestrant (50 µM) at 5 dpf for 5 hours. n=130, 110, 8. $p<0.0001$ between estradiol and estradiol + fulvestrant, by Fisher exact testing. (B) Co-treatment of mestranol (2.5 µM) and fulvestrant (25 µM) at 3 dpf for 48 hours. n=69 and 156. $p<0.05$ by Fisher exact testing. (C) Triple heterozygous *esr1*$^{+/-}$;*esr2a*$^{+/-}$;*esr2b*$^{+/-}$ mutants were incrossed and larvae treated with 5 µM mestranol at 3 dpf for 48 hours (n=21, 40, 20 for the *esr1*/*esr2a*$^{+/+}$ strata; 49, 92, 47 for the *esr1*/*esr2a*$^{+/-}$ strata; 26, 39, 26 for the *esr1*/*esr2a*$^{-/-}$ strata). Genotyping was performed after thrombosis quantification. Fisher exact testing revealed no significant differences. (D) Larvae from *gper*$^{+/-}$ incrosses were treated with 5 µM mestranol at 3 dpf for 48 hours. Genotyping was performed after thrombosis quantification. No difference was detected by Fisher exact testing, n= 40, 62, and 37. (E) STX(18) treatment at 3 dpf for 48 hours. No statistical significance observed among the groups (n=19, 17, 20, 20, 20). All data were

706 collected in the *fgb-egfp* transgenic background by an observer blinded to condition and/or
707 genotype.

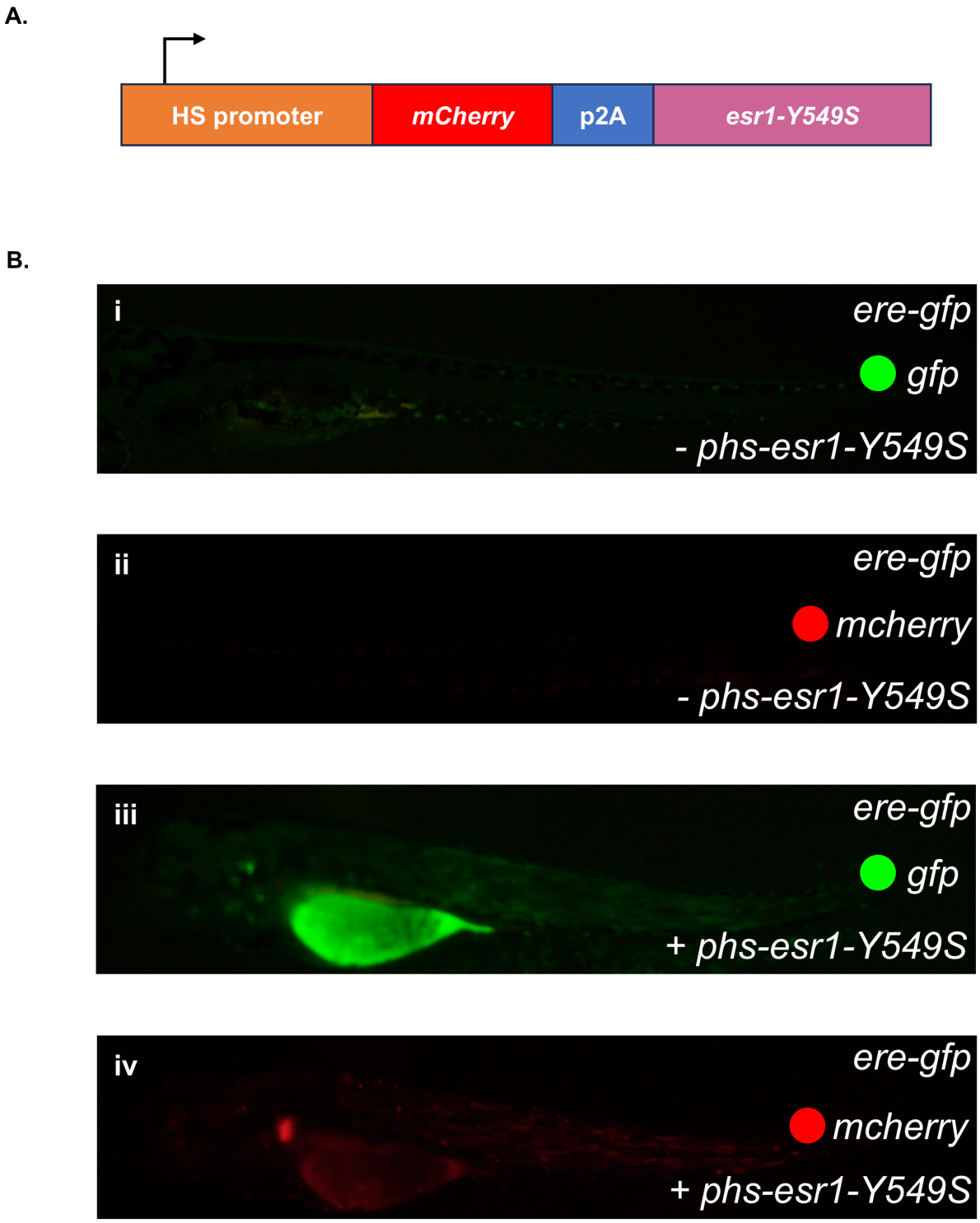

708

709 **Figure 7: Constitutively active nuclear hormone estrogen receptor does not induce**

710 **thrombosis.** (A) p*hs-esr1*-Y549S plasmid with constitutively active *esr1* (Y549S). Expression

711 was driven by the heat shock promoter (HS), along with *mcherry* followed by p2A and the mutant

712 *esr1* cDNA. (B) p*hs-esr1*-Y549S was injected into *fgb-egfp;ere-gfp* transgenic embryos, treated at
713 35ºC at 3 dpf, and evaluated at 5 dpf. GFP indicates activation of the estrogen response element
714 (ERE), and mCherry indicates expression from p*hs-esr1*-Y549S. (i-ii) Uninjected controls show
715 no ERE activity or mCherry expression. (iii-iv) Injected larvae show expression from p*hs-esr1*-
716 Y549S by activation of ERE and subsequent GFP signal, as well as expression of mCherry. Despite
717 evidence of constitutive *esr1* activity, no thrombosis was observed. All data were collected using
718 the *fgb-egfp* transgenic background by an observer blinded to condition.

719 # Tables

720 **Table 1. sgRNA sequences**

Description	Sequence (5’ → 3’)
esr1 sgRNA (exon 2)	CCGTATCTGAGCCATCACGG
esr1 sgRNA (exon 9)	GGAGAAAAGTTACTCTTAGA
esr2a sgRNA (exon 2)	ACACAGACCTTGGCCACGAC
esr2a sgRNA (exon 10)	CTCAAGTACTCACCAGTTCA
esr2b sgRNA (exon 1)	GTGTCCGAAAGCCTCGTCCC
esr2b sgRNA (exon 9)	TTGGCTGAGACAGTTACATA

721

722

723 **Table 2. Primer sequences for genotyping**

Gene	Forward (5’ → 3’)	Reverse 1 (5’ → 3’)	Reverse 2 (5’ → 3’)
esr1	GAGAGAGAAGCCCTGGAGGA	GTGCTGGACGAGGAATCCAG	TCACTGAGCAGTTTTTCCCCA
esr2a	CCCAGTATCGAGGACTGAGAAG	GACTGTAAAAGGGCAGAGTGCT	TAGCCAGCAGTAATGATGCT
esr2b	ATGCAGTAGTGTGTCAGGCC	TGTGTGAACGTGTTTCGCTG	ACCACGAAAAGCACTACAGGA

724

725

726